First-principle calculation of core level binding energies of Li x PO y N z solid electrolyte

Émilie Guille, Germain Vallverdu, and Isabelle Baraille

Articles you may be interested in

Biased interface between solid ion conductor LiBH4 and lithium metal: A first principles molecular dynamics study
Appl. Phys. Lett. **103**, 133903 (2013); 10.1063/1.4823503

Identification of boron clusters in silicon crystal by B1s core-level X-ray photoelectron spectroscopy: A first-principles study
Appl. Phys. Lett. **99**, 191901 (2011); 10.1063/1.3658030

Electronic structural and electrochemical properties of lithium zirconates and their capabilities of CO 2 capture: A first-principles density-functional theory and phonon dynamics approach
J. Renewable Sustainable Energy **3**, 013102 (2011); 10.1063/1.3529427

Core-level electronic structure of solid-phase glycine, glycyl-glycine, diglycyl-glycine, and polyglycine: X-ray photoemission analysis and Hartree–Fock calculations of their zwitterions
J. Chem. Phys. **129**, 105104 (2008); 10.1063/1.2976151

Predicting ionic conductivity of solid oxide fuel cell electrolyte from first principles
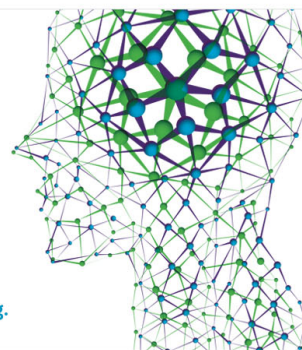J. Appl. Phys. **98**, 103513 (2005); 10.1063/1.2135889

CrossMark
click for updates

First-principle calculation of core level binding energies of $Li_xPO_yN_z$ solid electrolyte

Émilie Guille, Germain Vallverdu,[a)] and Isabelle Baraille
IPREM - ECP CNRS UMR 5254, Université de Pau et des Pays de l'Adour, Technopole Hélioparc,
2 Ave. du Président Pierre Angot, 64053 Pau cedex 9, France

We present first-principle calculations of core-level binding energies for the study of insulating, bulk phase, compounds, based on the Slater-Janak transition state model. Those calculations were performed in order to find a reliable model of the amorphous $Li_xPO_yN_z$ solid electrolyte which is able to reproduce its electronic properties gathered from X-ray photoemission spectroscopy (XPS) experiments. As a starting point, Li_2PO_2N models were investigated. These models, proposed by Du *et al.* on the basis of thermodynamics and vibrational properties, were the first structural models of $Li_xPO_yN_z$. Thanks to chemical and structural modifications applied to Li_2PO_2N structures, which allow to demonstrate the relevance of our computational approach, we raise an issue concerning the possibility of encountering a non-bridging kind of nitrogen atoms ($=N^-$) in $Li_xPO_yN_z$ compounds. © *2014 AIP Publishing LLC.* [http://dx.doi.org/10.1063/1.4904720]

I. INTRODUCTION

The increasing diversity of electronic portable devices implies a necessary thought on energy storage, those technologies being demanding in terms of lightness, size, and battery life. The use of solid electrolytes nowadays constitutes a possible response to those growing requirements, while it appears also as an alternative solution to the safety problems induced by the common use of liquid electrolytes in Li-ion batteries. Besides, reactivity towards the electrodes is lowered in the case of solid electrolytes, this parameter still being one of the Achilles' heels of liquid electrolytes. Indeed, a solid-liquid interface (SEI) forms at the interface between the electrode and the electrolyte during the charge and discharge cycles; this passivation layer appearing both essential for the protection of the electrode and limiting for Li-ion diffusion. Both formation and properties of SEI have been largely investigated in the case of liquid electrolytes, while it is not the case for solid electrolytes, which motivates research on the interfaces with the electrodes and constitutes the background of the present study.

Among solid electrolytes of interest appears the $Li_xPO_yN_z$ (where $x = 2y + 3z - 5$, $z \leq 1$) compound, widely studied from an experimental point of view[1–5] and otherwise already employed in commercial devices. Experimentally, the synthesis of thin films of $Li_xPO_yN_z$ is made by use of radio-frequency magnetron sputtering and starts from an amorphous form of γ-Li_3PO_4, this material being then submitted to an N_2/Ar flux.[6,7]

The present theoretical work aims at finding a structural model of this electrolyte, adapted to periodic density functional theory (DFT) calculations and able to reproduce the experimental electronic characteristics (X-ray photoemission spectroscopy (XPS) spectra) reported in the literature.[6] Indeed,

this study being part of a more extensive work which purpose lies in the modelling of electrode/$Li_xPO_yN_z$ interfaces, the first barrier to break consists in the search for a model of this amorphous electrolyte. Nevertheless, even though this electrolyte has been the subject of intensive research at the experimental level (XPS,[6–10] Raman,[11] high-performance liquid chromatography,[8] and nuclear magnetic resonance (NMR)[12]), it is not the case of its theoretical investigation. Du and Holzwarth[13] studied the nitrogen doping of Li_xPO_y compounds from the point of view of both thermodynamics and vibrational properties. Thanks to the computation of heats of formation, they evidenced the possibility of synthesizing a $Li_xPO_yN_z$ compound with a Li_2PO_2N chemical composition and predicted its vibrational properties. To our knowledge, Li_2PO_2N structures constitute the only periodic models proposed up to now, likely to represent the structure of real $Li_xPO_yN_z$ electrolytes. Thus, they were used as a starting point for the present study.

Moreover, the theoretical study of the electronic properties of $Li_xPO_yN_z$, particularly the computation of XPS core level spectra, has not yet been, to our knowledge, the subject of in-depth research, those latter mainly focusing on lithium ion diffusion within the electrolyte.[14–17] The computation of core-level binding energies in the case of periodic structures can be reached by application of[18] (i) the complete screening picture or (ii) the transition-state model. However, theoretical works available in the literature and referring to the calculation of binding energies involve metallic compounds, alloys or surfaces, while $Li_xPO_yN_z$ belongs to insulating, bulk phase, class of materials. Thus, by means of the investigation of Li_2PO_2N compounds as potential models of the electrolyte, the validity of the commonly used Slater-Janak transition state model for the computation of binding energies on such insulating materials is discussed.

The present paper is organized as follows: Sec. II presents the computational methods and conditions used; in Sec. III, we focus on crystalline Li_xPO_y compounds and made a compar-

---

a)Author to whom correspondence should be addressed. Electronic mail: germain.vallverdu@univ-pau.fr

141, 244703-1

ison between experimental and computed binding energies to check the validity of the computational approach. Section IV then gives the results of binding energy computations on Li_2PO_2N models. Starting from those structures, we evaluate the sensitivity of the computational method to the modification of the chemical environment surrounding the atom of interest, which is one of the specifications of the XPS technique. Finally, we discuss the theoretical approach proposed as well as the use of Li_2PO_2N models for the simulation of the electronic behavior of $Li_xPO_yN_z$ electrolyte.

II. METHOD FOR THE CALCULATION OF CORE LEVEL BINDING ENERGIES

A. Computational details

All calculations were performed using the plane wave DFT code available in the Vienna *Ab Initio* Simulation Package (VASP)[19,20] within the generalized gradient approximation, using the Perdew-Burke-Ernzerhof (PBE)[21] functional. The electronic wavefunctions were described in the Projected Augmented Wave (PAW) formalism,[22,23] and a realspace projection was further used for the total wavefunction analysis.

We checked the quality of the basis set by increasing the plane wave energy cut-off from 300 to 700 eV. The plane wave energy cut-off was set to 500 eV, which appeared to be a converged value for all of the crystalline systems studied. The Brillouin zone integration was done on a k-point grid distributed uniformly around the origin using a mesh of $4 \times 4 \times 4$. Cell parameters and atomic positions were fully relaxed.

Convergence on the eigenenergies is reached as far as electronic relaxation is allowed in a radius of about 4.0 Å around the atom of interest, to account for the final state effects (see supplementary material). In order to avoid spurious interactions between the core hole created all along the calculations, supercells of the materials investigated were considered. Dimensions of the supercells used for the whole materials studied are given in the supplementary material.[38]

B. Methodology

From an experimental point of view, getting XPS core level binding energies goes through the ejection of a core electron to the infinite under an X-ray irradiation. The energy difference between the incident photon and the kinetic energy of the ejected electron corresponds to the *core-level binding energy*. At the computational level, the ejection of a core level electron to the infinite leads to an ion, the treatment of which is not trivial in a periodic formalism. To circumvent this problem, Johansson and Mårtensson[24] proposed an approximation, best-known as the "*Z + 1 approximation*" on the basis of their study on metallic elements. They considered that the site from which the core electron is ejected is totally screened by the surrounding conduction electrons, so that one can artificially put the ejected electron into the conduction band without affecting the screening of the hole. Practically, a single core electron is excited from the core to the conduction band, by generating the corresponding core excited ionic PAW potential in the course of the *ab initio* calculations. Screening by the core electrons is

not taken into account (i.e., the other core electrons are kept frozen in the configuration for which the PAW potential was generated). Screening by the valence electrons is included, however.[25]

Getting an accurate core level binding energy computation goes through many factors, the main of which being the initial and final state approximations: the initial state contribution corresponds to the eigenenergy of a particular core electron before ionization while final state effects take into account the remaining contributions, especially the electronic relaxation. One of the most frequently used methods for binding energy computations is the model referred to as the Slater-Janak transition state model,[18,26] which includes both the initial and final state effects, as the most predominant factors. This method is based on the theorem by Janak,[27] which constitutes an extension of DFT by dealing with the partial occupation of electron levels

$$\frac{\partial E}{\partial \eta_i} = \epsilon_i(\eta_i), \qquad (1)$$

where η_i stands for the partial occupation number of the core orbital i of interest ($0 \leq \eta_i \leq 1$), E corresponding to the total electronic energy. By integration of Eq. (1), it becomes possible to connect the initial state (N) and the final state ($N - 1$) by removing $(1 - \eta_i)$ electrons from the core orbital i[26,27]

$$E_{N-1} - E_N = \int_1^0 \epsilon_i(\eta_i)d\eta_i = E_l, \qquad (2)$$

this integral corresponding to the binding energy of the electron i.

When the eigenenergy ϵ_i depends linearly upon the occupation number η_i, Eq. (2) could be written as

$$E_l \approx \epsilon_i(1) + \frac{1}{2}(\epsilon_i(0) - \epsilon_i(1)) = \epsilon_i(1/2). \qquad (3)$$

If the curves $\epsilon_i = f(\eta_i)$ are perfectly linear, E_l can be reached through the computation of $\epsilon_i(1/2)$ which corresponds to the eigenenergy obtained when considering an half-occupation of the orbital i of interest. The accuracy of such an approximation thus depends on the linearity of the curves $\epsilon_i = f(\eta_i)$ (depicted in Figure 1).

The suitability of the use of Eq. (3) for the computation of core-level binding energies has been tested, in the case of both N1s and O1s core orbitals, on several systems of interest for this study and at several levels of approximation. Table I presents $\epsilon_i(1/2)$ and the value of the numerical integration of Eq. (2), which take into account the final state contributions and $\epsilon_i(1)$, which exclusively accounts for initial state effects.

Considering $\epsilon_i(1)$ in the Koopmans' formalism, it can be noted that initial state effects lead to a good reproduction of the qualitative behavior. Nevertheless, a deviation of about 30 eV is obtained in comparison with experimental values of N1s and O1S binding energies, 397.0 eV and 532.6–534.5 eV, respectively.

Getting reasonable quantitative values necessarily requires the consideration of final state effects. In this case, the use of $\epsilon_i(1/2)$ leads to an error, on the approximation of the integral in Eq. (2), comprised between 0.2 and 1.4 eV, depending on both the system and the core state considered. Those errors can be attributed to the deviation from linearity
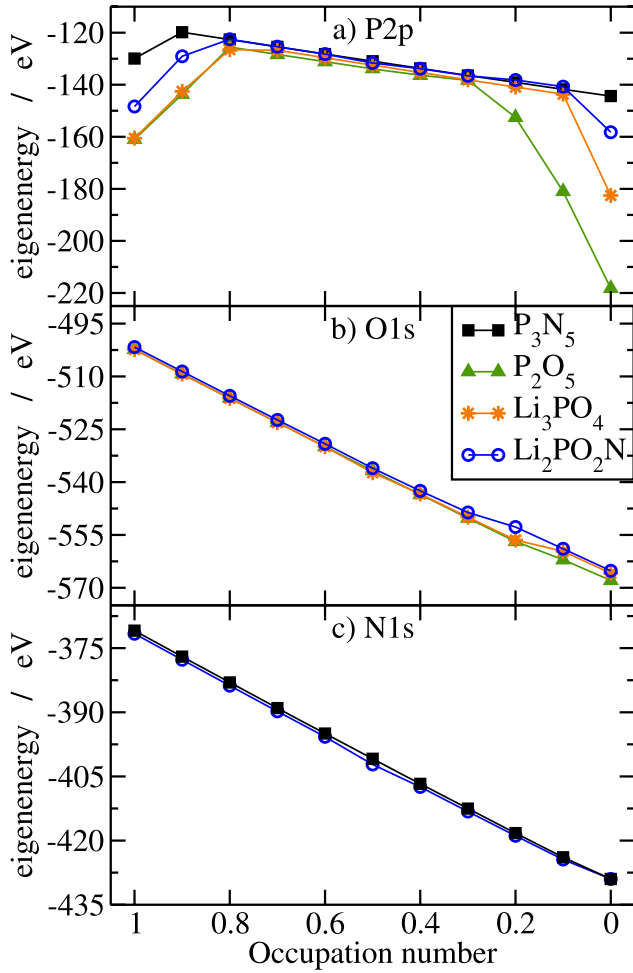
FIG. 1. $\epsilon_i = f(\eta_i)$ for the following core orbitals: (a) P2p; (b) O1s; (c) N1s.

of the curves $\epsilon_i = f(\eta_i)$. In the literature, the deviation from linearity is evaluated by Göransson *et al.*[28] through the following parameter:

$$D = \frac{\Delta}{|\epsilon_i(0) - \epsilon_i(1)|} , \qquad (4)$$

where

$$\Delta = \frac{1}{N}\sqrt{\sum_{i=0}^{n}[\epsilon(\eta_i)^{int.} - \epsilon(\eta_i)^{calc}]^2} \qquad (5)$$

is the norm of residuals, with $\epsilon(\eta_i)^{int.}$ the linearly interpolated value of the eigenenergy, $\epsilon(\eta_i)^{calc}$ the eigenenergy from first-principle calculations, and N the number of sampling points. This way of evaluating D allows a comparison between the core levels studied. According to the values calculated on the systems of interest and reported in Table I, it appears that D is systematically lower than the values reported in the literature,[28] which tends to suggest the validity of such a method for the study of $Li_xPO_yN_z$ compounds. Indeed, studies implying XPS core-level calculations only relate, to our knowledge, to surface and interface issues[25,29–31] or metals and alloys.[26,28,32] In the present case, we only consider bulk phases of non-metallic electronic behaviors, for which the validity of the approximation used in Eq. (3) was not trivial. However, despite the linear behavior of the curves $\epsilon_i = f(\eta_i)$, as estimated through D, the error committed while considering the approximation used in Eq. (3) is of about 1 eV, as previously highlighted. Although it corresponds to a relative error which may not exceed 0.2%, it also corresponds to the order of magnitude of the chemical displacements we aimed at simulate.[6]

However, the computation of binding energies through Eq. (3) does not take into account some significant experimental parameters, among which, as the major contribution, the workfunction of the material of interest. To account for this workfunction and then directly compare between computed and experimental core-level binding energies, we used the following equation:

$$BE_{i,corr}^{mat} = BE_{i,exp}^{ref} + (\epsilon_{i,calc}^{mat} - \epsilon_{i,calc}^{ref}) \qquad (6)$$

in which: $BE_{i,exp}^{ref}$ stands for the experimental binding energy related to the core orbital i of interest, in a reference material; $\epsilon_{i,calc}^{mater}$ and $\epsilon_{i,calc}^{ref}$ stand for the computed eigenenergies of the core orbital i of interest in the material studied and in the reference material, respectively. Equation (6) involves a reference material that allows to account for the workfunction of the material studied, as this parameter is included in the energy difference $BE_{i,exp}^{ref} - \epsilon_{i,calc}^{ref}$. Indeed, as long as the reference material and the material of interest show close electronic and structural properties, their respective workfunctions can be supposed as equivalent, so that the workfunction of the material studied is effectively taken into account.

Equation (6) leads to absolute core-level binding energies, allowing for a direct comparison between computed values and experimental XPS data. Besides, the $\epsilon_{i,calc}^{mat} - \epsilon_{i,calc}^{ref}$ term

TABLE I. Evaluation of the deviation from linearity of the curves $\epsilon_i = f(\eta_i)$ on several compounds of interest: (i) through the calculation of the D parameter[28] and (ii) through the comparison of the numerical integration (Num. Int.) of Eq. (2) with its approximation by $\epsilon_i(1/2)$ (Eq. (3)). Values of $\epsilon_i(1)$ are also given to estimate the initial state effects. All reported values are given in eV, with the exception of D which has no unit.

| System | Core state | D | E_l Eq. (3) | | | $\|\epsilon_{i,calc}^{mat} - \epsilon_{i,calc}^{ref}\|$ Eq. (6) | |
			$\epsilon_i(1)$	$\epsilon_i(1/2)$	Num. int.	$\epsilon_i(1/2)$	Num. int.
P_2O_5	O1s	0.003	−502.33	−536.76	−536.30		
P_3N_5	N1s	0.002	−370.92	−400.87	−400.64		
γ-Li_3PO_4	O1s	0.006	−502.36	−537.35	−535.92	0.59	0.38
Li_2PO_2N	O1s	0.005	−501.67	−536.06	−534.83	0.70	1.47
	N1s	0.003	−371.63	−402.20	−401.45	1.33	0.81

minimizes the systematic computational errors. In particular, the error of 1 eV, as previously pointed out when using Eq. (3), is minimized. Thanks to compensation of errors, the use of Eq. (6) implies an effective error of 0.5 eV in the computation of N1s core-level binding energies (cf. Table I). This error corresponds to the energy difference between the values calculated for the term $\epsilon_{i,calc}^{mat} - \epsilon_{i,calc}^{ref}$ using the eigenenergy computed for an half-occupation of the core orbital i ($\epsilon_i(1/2)$ term) on the one hand and using the numerical integration of Eq. (2) on the other hand. As this work focuses on N1s core peaks, calculated core-level binding energies will have to be considered with a margin of error of 500 meV. This error appears larger compared to the 100 to 200 meV of error reported in the literature.[29,30]

Reference materials have been chosen for their structural and electronic similarities with the systems of interest. Indeed, as the XPS technique is very sensitive to the chemical environment surrounding each atom, reference materials have to be judiciously chosen. We made the choice of defining a given reference material for each kind of chemical environment observed thanks to XPS analysis on $Li_xPO_yN_z$ materials:

1. P_2O_5 for O1s and P2p core orbitals in a bridge type environment (P–O–P);
2. P_3N_5 for N1s and P2p core orbitals in a bridge type environment (P–N–P);
3. KH_2PO_4 for the particular case of a P2p and O1s core orbitals in a tetrahedral type environment (PO_4^{3-}).

Computed eigenenergies as well as structural data corresponding to the reference materials are given in the supplementary material and will be used for each of the binding energy calculations done all through this paper due to the application of Eq. (6).

Focusing on the case of P2p core states, which has not yet been discussed, one can note that the curves $\epsilon_i = f(\eta_i)$ associated with P2p core orbitals depict significant deviations to the linearity. This result is consistent with the trends noticed by Göransson et al.[28] and Olovsson et al.,[32] which show that the deeper the energy of the core state, the more linear the curve $\epsilon_i = f(\eta_i)$ is, due to a better screening of the core hole. In the case of P2p core states, we will thus only discuss on the relative positions of computed binding energies, with no consideration of their absolute values. Indeed, beyond the non-linearity of the curves associated with P2p core orbitals, computed eigenenergies (see supplementary material[38]) are always such as $\epsilon_i^{P_3N_5} > \epsilon_i^{Li_3PO_4} > \epsilon_i^{P_2O_5}$, whatever occupation number considered, in agreement with experimental data, allowing to further consider the computed P2p binding energies from a qualitative point of view. It has to be noted that we did not take into account the spin-orbit coupling, so that computed P2p binding energies will be compared, in the following study to the experimental range between the two peaks, respectively, associated with the 1/2 and 3/2 components.

III. RESULTS

A. Li_xPO_y crystalline structures

In order to evaluate the suitability of our computational approach, we considered three crystalline Li_xPO_y structures

and computed their P2p and O1s binding energies for a comparison with the corresponding available experimental data. We chose the following Li_xPO_y compounds (depicted in Figure 2):

- γ-Li_3PO_4, target material for the synthesis of $Li_xPO_yN_z$ and exclusively made of isolated phosphate tetrahedra.
- $Li_4P_2O_7$, constituted of phosphate dimers
- $LiPO_3$, made of infinite phosphate chains.

Note that the structural data associated with the crystalline structures studied throughout this work are available in the supplementary material.[38]

The choice of those three Li_xPO_y structures also allows to evaluate the sensitivity of binding energy computations to the environment. Indeed, each of those compounds displays a particular tetrahedral organization, that is to say a distinctive pattern in the first coordination sphere surrounding phosphorus atoms. Therefore, the analysis of P2p core peaks should give information about the core peak shift when modifying the nature of the chemical bonds in the first coordination sphere (see Figure 2 and Table II).

Results of binding energy computations are reported in Table III. Experimental binding energies for γ-Li_3PO_4 have been taken from the results by Fleutot et al.[6] and precisely refer to their so-called *LiPON*-0 as it corresponds to a vitreous form of γ-Li_3PO_4. Experimental data for $Li_4P_2O_7$ refer to the work by Chowdari et al.,[33] whereas values associated with $LiPO_3$ crystalline structure have been collected in our group.

Experimental data highlight the sensitivity of the XPS technique to the modification of the chemical bond in the first coordination sphere. Indeed, P2p core peaks appear shifted towards higher energies when bridging oxygen atoms enter in their first coordination sphere. Compared to γ-Li_3PO_4, in which phosphorus atoms are exclusively bonded to non-bridging kinds of oxygen atoms, the P2p core peak associated with $LiPO_3$ structure is experimentally shifted by +1.9 eV.

All computed binding energies appear to fall within the experimental range when considering the uncertainties, both associated with the computational method used and the experiment. Particularly, O1s core peaks appear properly reproduced, both qualitatively and quantitatively when taking into account the uncertainties. In the case of γ-Li_3PO_4, three types of non-equivalent oxygen atoms can be encountered, but their environment in the two first coordination spheres is equivalent and so do their eigenenergies, which differ by no more than 0.02 eV.

We made the choice of treating P2p core peaks as N1s and O1s ones, by computing $\epsilon_i(1/2)$, even though this way of evaluation implies a larger error. Computations of P2p binding energies appear to lead to a good qualitative agreement, as the respective positions of the peaks calculated for those three structures generally reproduce the experimental trend. Despite an overestimation of the P2p binding energy in the case of γ-Li_3PO_4, we found a computed value for $Li_4P_2O_7$ that falls close to the 1/2 component associated with the γ-Li_3PO_4 structure. Calculation then predict a shift of +1 eV between those two structures and $LiPO_3$. Thus, even if the shift amplitude is, on the whole, underestimated compared to the experiment, the computed values are sufficiently different
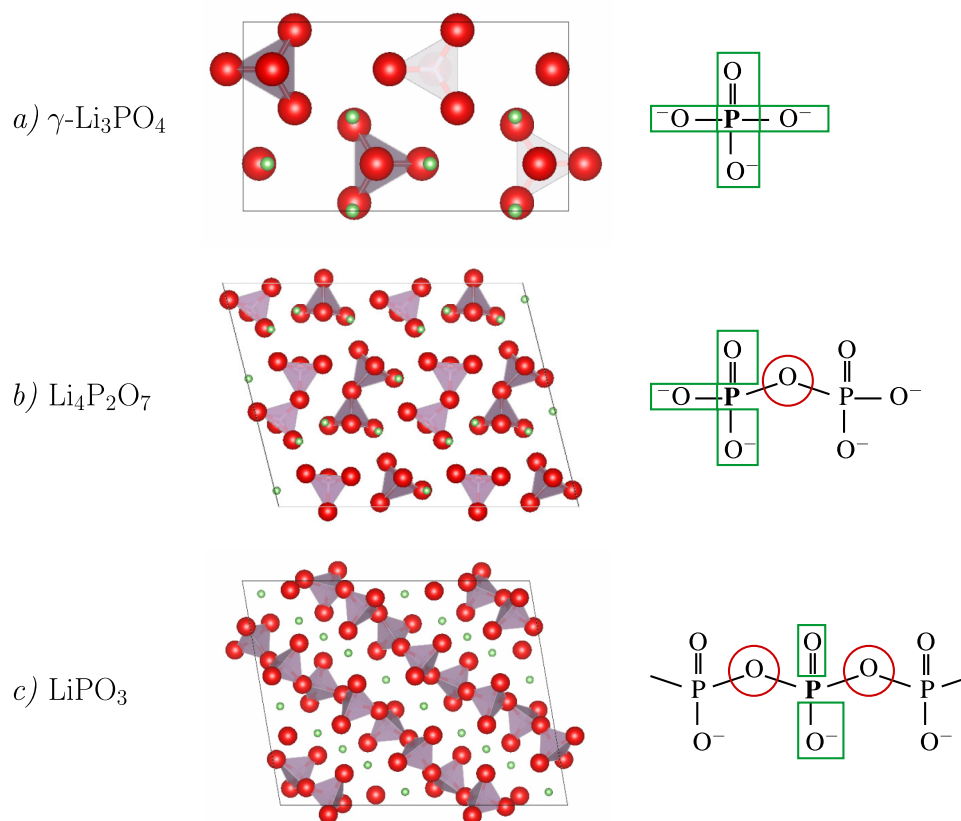
FIG. 2. Crystalline Li_xPO_y structures versus a Lewis representation of the respective environments around phosphorus atoms. (a) γ-Li_3PO_4, (b) $Li_4P_2O_7$, and (c) $LiPO_3$. Red, green, and purple spheres refer to oxygen, lithium, and phosphorus atoms, respectively. On lewis representations, green rectangles and red circles evidence bridging and non-bridging oxygen atoms.

to reasonably validate our computational approach as from a qualitative point of view, the experimental behavior is satisfactorily reproduced. The suitability of the computational method on such systems is reinforced by its sensitivity to the nature of the chemical bonds in the first coordination sphere, which constitutes a specific feature of the XPS technique.

Considering the close electronic behavior on Li_xPO_y and $Li_xPO_yN_z$ systems, we can make the reasonable assumption

that this theoretical approach will also be well-adapted to the study of $Li_xPO_yN_z$ type of structures. On this basis, we will then present the investigations we made on Li_2PO_2N systems.

B. Li₂PO₂N models

Li_2PO_2N systems have been proposed by Du and Holzwarth[13] as original $Li_xPO_yN_z$ potential systems (see Figure 3). Three models of the same chemical composition have been created, all based on the doping of a symmetrized

TABLE II. First neighbors surrounding the phosphorus atom chosen for the binding energy calculation, for each Li_xPO_y structure: *(nb)* stands for non-bridging oxygen atoms, whereas *(b)* refers to bridging oxygen atoms.

Structure	Coordination sphere	Number	Type	Distance (Å)
γ-Li_3PO_4	1st	4	O *(nb)*	1.53-1.55
	2nd	5	Li	2.95-3.02
$Li_4P_2O_7$	1st	3	O *(nb)*	1.42-1.54
		1	O *(b)*	1.65
	2nd	1	O	2.94
		1	Li	3.01
$LiPO_3$	1st	2	O *(nb)*	1.50
		2	O *(b)*	1.61-1.62
	2nd	1	Li	2.89
		1	P	2.94

TABLE III. Computed facing experimental core level binding energies (BE, in eV) of O1s and P2p core orbitals of γ-Li_3PO_4, $Li_4P_2O_7$, and $LiPO_3$; *(nb)* stands for non-bridging oxygen atoms whereas *(b)* refers to bridging ones. Reference materials for the calculations are labeled as follows: (∗) KH_2PO_4 (P2p), (†) KH_2PO_4 (O1s, P–O⁻ ⁺Li), (‡) P_2O_5 (P2p), (§) P_2O_5 (O1s), and (¶) P_2O_5 (O1s, P=O).

Structure	BE	P2p	O1s *(nb)*	O1s *(b)*
γ-Li_3PO_4	Expt.[6]	132.9 – 133.8	532.5	
	computed	134.5[(∗)]	533.1[(†)]	
$Li_4P_2O_7$	Expt.[33]	133.7	531.4	533.1
	computed	134.3[(‡)]	531.7[(¶)]	533.8[(§)]
$LiPO_3$	Expt.	134.8 – 135.6	532.2	533.7
	computed	135.3[(‡)]	532.8[(†)]	533.9[(§)]

a) s1-Li$_2$PO$_2$N

b) s2-Li$_2$PO$_2$N

c) s3-Li$_2$PO$_2$N

FIG. 3. Representations of the three Li$_2$PO$_2$N models:[13] (a) s1, (b) s2, and (c) s3.

TABLE IV. Computed O1s, N1s, and P2p core orbital energies (BE, in eV) for all of the three Li$_2$PO$_2$N compounds; the experimental data correspond to the Li$_{3.25}$PO$_{3.00}$N$_{1.00}$ composition; *(nb)* refers to non-bridging oxygen atoms. Reference materials for the calculations are labeled as: (†) KH$_2$PO$_4$ (O1s, P–O$^-$ $^+$Li), (‖) P$_3$N$_5$ (N1s), and (¶) P$_2$O$_5$ (P2p).

Structure	O1s *(nb)*	N1s	P2p
s1-Li$_2$PO$_2$N	534.4$^{(†)}$	395.7$^{(‖)}$	132.3$^{(¶)}$
s2-Li$_2$PO$_2$N	534.4$^{(†)}$	395.7$^{(‖)}$	132.4$^{(¶)}$
s3-Li$_2$PO$_2$N	533.2$^{(†)}$	394.7$^{(‖)}$	131.3$^{(¶)}$
Expt.[6]	532.3	397.9	132.8 – 133.8

able to reproduce its electronic properties, Li$_2$PO$_2$N models were considered as a starting point for our investigations. As a basis, we computed their binding energies (cf. Table IV) in order to compare those gathered data with the corresponding experimental XPS spectra of a real Li$_x$PO$_y$N$_z$.[6]

All of the three Li$_2$PO$_2$N models fail to simultaneously reproduce the experimental O1s, N1s, and P2p binding energies. Particularly, it is noticeable from the analysis of computed binding energies that they do not properly reproduce the environments around nitrogen atoms, as the calculated values for the N1s core orbital deviates from the experiment by much than 2 eV.

Thus, even when taking into account the uncertainties, none of the calculated binding energies appears in agreement with the experiment, so that Li$_2$PO$_2$N systems cannot be used as models for the simulation of the electronic properties of Li$_x$PO$_y$N$_z$ electrolyte.

Nevertheless, one can note that the structure labeled s3 behaves differently from s1 and s2, which suggests slight structural differences between those systems. In fact, while in s1 and s2 all tetrahedral units appear oriented in the same way, and in s3 they are all twisted by 90° relative to each other.[13] An analysis of the first neighbors around each kind of atoms should then reveal this particular structuration. Table V reports the list of first neighbors that surrounds the phosphorus atom used for the binding energy computation, for each Li$_2$PO$_2$N system. This structural analysis reveals that, while s1 and s2 systems present exactly the same environments in their three first coordination spheres, s3 shows a distinctive structural pattern. Indeed, a lithium atom enters in its second coordination sphere, suggesting that this latter plays a significant role in the core peak position.

Based on those results, which tend to demonstrate that Li$_2$PO$_2$N models cannot be used to simulate the electronic properties of the real Li$_x$PO$_y$N$_z$ electrolyte, we tried to improve those systems by applying two kinds of modifications, namely,

- a modification of their chemical composition, by varying the nitrogen rate from $z = 1$ to $z = 0.5$;
- a structural modification, by putting half of the nitrogen atoms into a non-bridging position, the bridging atoms moved being replaced by oxygen ones.

Those modifications should also allow to evaluate the influence of those factors on the shift of the N1s core peak. In particular, as suggested by the structural analysis done on s1,

LiPO$_3$ structure in which all bridging oxygen atoms were substituted by nitrogen ones. The three systems obtained, labeled s1, s2, and s3-Li$_2$PO$_2$N, differ from one another by the orientation of the phosphate chains within the cell. As the present paper is taken part in an extensive study on the search for a suitable model of the amorphous electrolyte Li$_x$PO$_y$N$_z$,

TABLE V. Coordination sphere, number (#), types, and distances of the first neighbors surrounding the nitrogen atom used for binding energy calculations, in the case of Li_2PO_2N, $Li_{1.5}PO_{2.5}N_{0.5}$, and structurally modified systems.

		Li_2PO_2N				$Li_{1.5}PO_{2.5}N_{0.5}$				$(Li_2PO_2N)_{mod.}$		
	Sphere	#	Type	Distances (Å)	Sphere	#	Type	Distances (Å)	Sphere	#	Type	Distances (Å)
s1	1st	2	P	1.63	1st	2	P	1.59-1.60	1st	2	P	1.60-1.65
	2nd	1	Li	2.01	2nd	1	Li	1.96	2nd	2	Li	2.01-2.15
	3rd	2	O	2.59-2.63	3rd	3	O	2.54-2.59	3rd	2	O	2.59-2.61
	3rd	1	N	2.63								
s2	1st	2	P	1.63	1st	2	P	1.60-1.66	1st	2	P	1.61-1.66
	2nd	1	Li	2.01	2nd	1	Li	2.07	2nd	2	Li	2.04-2.06
	3rd	2	O	2.59-2.63	3rd	2	O	2.59-2.62	3rd	2	O	2.59-2.60
		1	N	2.63		1	N	2.63				
s3	1st	2	P	1.62-1.63	1st	2	P	1.61	1st	2	P	1.62-1.65
	2nd	2	Li	2.03	2nd	1	Li	2.02	2nd	2	Li	2.08-2.12
	3rd	1	N	2.56	3rd	3	O	2.59-2.61	3rd	2	O	2.52-2.54
		1	O	2.61								

s2, and s3 systems, we will be able to test the sensitivity of the core peak position to the chemical environment in the second and third coordinations spheres around the atom of interest.

These structural modifications were done for each of the s1, s2, and s3-Li_2PO_2N structures. The three new structures obtained were then fully relaxed.

1. Modification of the chemical composition: $Li_{1.5}PO_{2.5}N_{0.5}$

Li_2PO_2N structures were modified by dividing the nitrogen rate z by a factor two. In order to keep the neutrality of the model, we removed the corresponding amount of lithium atoms, so as to lead to a $Li_{1.5}PO_{2.5}N_{0.5}$ stoichiometry. As depicted in Figure 4 and following the deductions that can be made from the comparison of the structural analysis of Li_2PO_2N and $Li_{1.5}PO_{2.5}N_{0.5}$ (cf. Table V) systems, the modification of the nitrogen rate implies modifications on the nature of the chemical bond in the third coordination sphere around nitrogen atoms.

Figure 5 shows the computed N1s core peaks for both Li_2PO_2N and $Li_{1.5}PO_{2.5}N_{0.5}$ systems. Computed N1s core peaks obtained on $Li_{1.5}PO_{2.5}N_{0.5}$ structures all fall within the computational error associated with the computed core peaks of Li_2PO_2N models. This evidences that the modification of the nature of the chemical bond inside the third coordination sphere around the atom of interest is of no significant influence on the N1s core peak position. This result appears in good agreement with the experiment,[6] suggesting that the sensitivity of the experimental technique is satisfactorily reproduced.

2. Structural modification: Comments on the $=N^{-}{}^{+}Li$ coordinence

We modified the Li_2PO_2N models by introducing non-bridging nitrogen atoms, so as to lead to structures made of both bridging and non-bridging nitrogen atoms. Those structural modifications, which do not modify the chemical composition of the models, simply consisted in the inversion

of the positions of half of the nitrogen atoms with those of non-bridging oxygen ones, as represented in Figure 6.

Binding energy computations have been done exclusively on divalent nitrogen atoms as calculation of N1s and P2p core peaks associated with non-bridging nitrogen atoms require an adapted reference material, with a well characterized $P=N^{-}$ environment. To our knowledge, such a coordinence has not yet been characterized experimentally in the case of nitrogen atoms involved in a P–N bonding. Thus, we have no
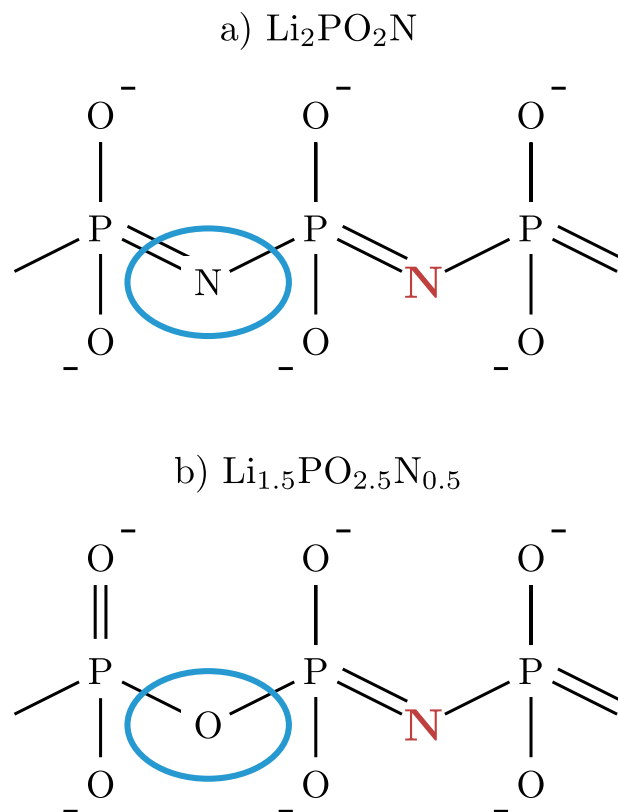

FIG. 4. Schematic representation of the effects of a chemical modification (in blue) on the second coordination sphere around a bridging nitrogen atom (in red): (a) Li_2PO_2N and (b) $Li_{1.5}PO_{2.5}N_{0.5}$.
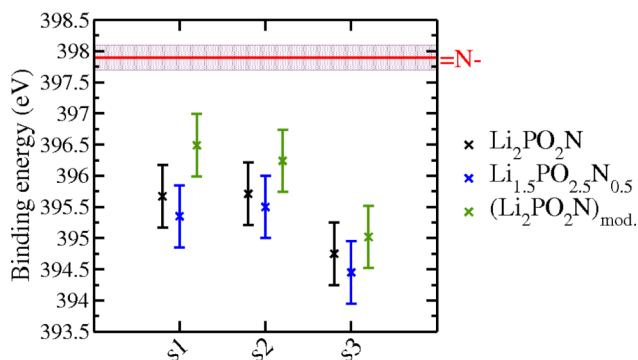
FIG. 5. Computed N1s core peaks of Li_2PO_2N (black), $Li_{1.5}PO_{2.5}N_{0.5}$ (blue), and structurally modified structures (green); red line stands for the experimental binding energy and its corresponding uncertainty.

TABLE VI. Absolute values of the computed eigenenergies ($\epsilon_{i,calc.}^{mat}$) of s1, s2, and s3-Li_2PO_2N compounds in the case of N1s core orbitals (eV): N1s (=N−) refers to divalent nitrogen atoms whereas N1s (=N−) refers to non-bridging nitrogen atoms.

Structure	N1s (=N−)	N1s (=N−)
s1-Li_2PO_2N	401.39	399.83
s2-Li_2PO_2N	401.63	399.89
s3-Li_2PO_2N	402.86	401.27

reference material available to be used for the calculation of the corresponding N1s core peak. However, the absolute values of the eigenenergies computed by VASP, referred to as $\epsilon_{i,calc.}^{mat}$ in Eq. (6), give the position of the N1s core peak of non-bridging nitrogen atoms with respect to divalent ones. Indeed, the formula applied to obtain core peaks (Eq. (6)) shall not change the relative positions observed on the computed eigenenergies. The corresponding absolute values for the eigenenergies are reported in Table VI. N1s core peaks associated with non-bridging nitrogen species are predicted to appear at lower

energy compared to divalent (P=N-P) nitrogen atoms (cf. Table VI). In fact, as the environment around the nitrogen atom (P=N−) is electron enriched, it implies that it will require lesser energy to extract a N1s core electron, so that the corresponding binding energy will be lowered compared to divalent (=N−) nitrogen atoms.

Compared to the chemical modification considered hereinabove, we applied there a structural modification inside the second coordination sphere around nitrogen atoms, as can be seen from the comparison of neighbors lists with the original Li_2PO_2N systems given in Table V.

From the observation of Figure 5, it appears that the main point to be discussed is the shift of the N1s core peak of divalent nitrogen atoms further to the insertion of non-bridging nitrogen atoms. A detailed analysis of the first neighbors around the nitrogen atom of interest (cf. Table V) reveals that, for each structure, the presence of non-bridging nitrogen atoms implies the insertion of a lithium atom in the second coordination sphere. This lithium atom, attracted by the charged nitrogen P=N− atom, enters in the close neighborhood of divalent nitrogen atoms and modifies the nature of the chemical interactions. The shift of the position of the N1s core peak thus demonstrates again the influence of the chemical environment in the second coordination sphere surrounding the atom studied.

Nevertheless, the amplitude observed for the shift of the N1s core peak differs between s1, s2, and s3. The structural analysis highlights that s3 is the only structure on which the structural modification applied do not lead to modifications in the second coordination sphere, but in the third. In agreement with the conclusions previously drawn on $Li_{1.5}PO_{2.5}N_{0.5}$ systems, this does not conduct to a significant shift of the core peak position.

Starting from those observations, both the presence of non-bridging nitrogen atoms and its structural consequences conduct to a shift of the divalent N1s core peak. Even if the real influence of non-bridging nitrogen atoms will need further evidences, as the structural reorganization that follows its addition is also of great importance, this kind of nitrogen atoms in the direct environment of a divalent nitrogen atom appears likely to shift the core peak position in the right direction. Besides, although not considered so far, this nitrogen coordence is chemically realistic. Indeed, ionic bonds likely to form with lithium ions (=N− +Li) in the real $Li_xPO_yN_z$ system are stable, although –O− +Li interactions are stronger and actually little more stable. Thus, there is no argument in disfavor of the existence of this coordence in the amorphous state, from an energetical point of view, even

a) Li_2PO_2N
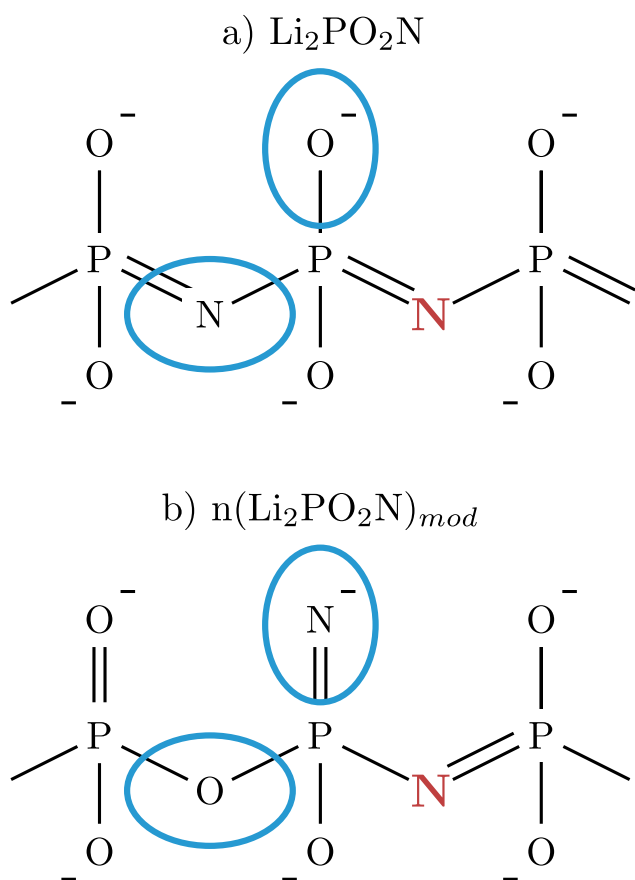

b) $n(Li_2PO_2N)_{mod}$

FIG. 6. Schematic representation of the effects of a chemical modification (in blue) on the second coordination sphere around a bridging nitrogen atom (in red): (a) Li_2PO_2N and (b) $(Li_2PO_2N)_{mod}$.

in a small amount when compared to other nitrogen coordinences. Furthermore, such an oxidation degree has already been observed for nitrogen atoms on oxynitride glasses[34–36] in Si–N⁻–Si kind of environment.

IV. CONCLUSIONS

The present work highlights the validity of the Slater-Janak transition-state model for the computation of binding energies in the case of insulating, bulk phase materials such as the Li_xPO_y and $Li_xPO_yN_z$ systems studied. The reliability of our computational approach has been tested on crystalline Li_xPO_y compounds for which computed binding energies appear in good agreement with the experiment. Besides, structural modifications applied on Li_2PO_2N systems highlighted the ability of the computational method used to simulate the XPS sensitivity. Thanks to gathered data, we demonstrated that only the first and second coordination spheres around the atom of interest have a significant influence on its core peak position. Those results are in relatively good agreement with the experimental studies by Fleutot *et al.*[6,7]

From the computed binding energies obtained on Li_2PO_2N compounds, we evidenced that those models cannot constitute reliable models for the study of the electronic properties of the real $Li_xPO_yN_z$ system, while we may have evidenced a way to improve them. Indeed, structural modifications, by means of the introduction of non-bridging (P=N⁻) nitrogen atoms, appeared to affect the N1s core peak position of bridging nitrogen atoms, so as to raise the issue of the possible existence of such a coordinence. This issue will be the subject of an extensive study involving the computation of binding energies, Raman spectra, and thermodynamic data in a confrontation between theory and experiment.

ACKNOWLEDGMENTS

[1]J. B. Bates, N. J. Dudney, G. R. Gruzalski, R. A. Zuhr, A. Choudhury, C. F. Luck, and J. D. Robertson, in *Proceedings of the 6th International Meeting on Lithium Batteries* J. Power Sources **43**, 103 (1993).
[2]N.-S. Roh, S.-D. Lee, and H.-S. Kwon, Scr. Mater. **42**, 43 (1999).
[3]C. H. Choi, W. I. Cho, B. W. Cho, H. S. Kim, Y. S. Yoon, and Y. S. Tak, Electrochem. Solid-State Lett. **5**, A14 (2002).
[4]H. Y. Park, S. C. Nam, Y. C. Lim, K. G. Choi, K. C. Lee, G. B. Park, S.-R. Lee, H. P. Kim, and S. B. Cho, J. Electroceram. **17**, 1023 (2006).
[5]Y. Hamon, A. Douard, F. Sabary, C. Marcel, P. Vinatier, B. Pecquenard, and A. Levasseur, Solid State Ionics **177**, 257 (2006).
[6]B. Fleutot, B. Pecquenard, H. Martinez, M. Letellier, and A. Levasseur, Solid State Ionics **186**, 29 (2011).
[7]B. Fleutot, B. Pecquenard, H. Martinez, and A. Levasseur, Solid State Ionics **206**, 72 (2012).
[8]B. Wang, B. C. Chakoumakos, B. C. Sales, B. S. Kwak, and J. B. Bates, J. Solid State Chem. **115**, 313 (1995).
[9]S. Jacke, J. Song, G. Cherkashinin, L. Dimesso, and W. Jaegermann, Ionics **16**, 769 (2010).
[10]B. Wang, B. S. Kwak, B. C. Sales, and J. B. Bates, J. Non-Cryst. Solids **183**, 297 (1995).
[11]T. Pichonat, C. Lethien, N. Tiercelin, S. Godey, E. Pichonat, P. Roussel, M. Colmont, and P. A. Rolland, Mater. Chem. Phys. **123**, 231 (2010).
[12]F. Munoz, A. Duran, L. Pascual, L. Montagne, B. Revel, and A. Rodrigues, Solid State Ionics **179**, 574 (2008).
[13]Y. A. Du and N. A. W. Holzwarth, Phys. Rev. B **81**, 184106 (2010).
[14]H. Rabaâ, R. Hoffmann, N. C. Hernández, and J. F. Sanz, J. Solid State Chem. **161**, 73 (2001).
[15]Y. Du and N. Holzwarth, Phys. Rev. B **76**, 174302 (2007).
[16]N. Holzwarth, N. Lepley, and Y. A. Du, J. Power Sources **196**, 6870 (2011).
[17]K. Senevirathne, C. S. Day, M. D. Gross, A. Lachgar, and N. A. W. Holzwarth, Solid State Ionics **233**, 95 (2013).
[18]W. Olovsson, T. Marten, E. Holmström, B. Johansson, and I. A. Abrikosov, J. Electron Spectrosc. Relat. Phenom. **178-179**, 88 (2010).
[19]G. Kresse and J. Hafner, Phys. Rev. B **47**, 558 (1993).
[20]G. Kresse and J. Furthmüller, Comput. Mater. Sci. **6**, 15 (1996).
[21]J. P. Perdew, K. Burke, and M. Ernzerhof, Phys. Rev. Lett. **77**, 3865 (1996).
[22]P. E. Blöchl, Phys. Rev. B **50**, 17953 (1994).
[23]G. Kresse and D. Joubert, Phys. Rev. B **59**, 1758 (1999).
[24]B. Johansson and N. Mårtensson, Phys. Rev. B **21**, 4427 (1980).
[25]L. Köhler and G. Kresse, Phys. Rev. B **70**, 165405 (2004).
[26]W. Olovsson, C. Göransson, L. Pourovskii, B. Johansson, and I. Abrikosov, Phys. Rev. B **72**, 064203 (2005).
[27]J. F. Janak, Phys. Rev. B **18**, 7165 (1978).
[28]C. Göransson, W. Olovsson, and I. Abrikosov, Phys. Rev. B **72**, 134203 (2005).
[29]A. Gandubert, E. Krebs, C. Legens, D. Costa, D. Guillaume, and P. Raybaud, Catal. Today **130**, 149 (2008).
[30]S. Lizzit, A. Baraldi, A. Groso, K. Reuter, M. Ganduglia-Pirovano, C. Stampfl, M. Scheffler, M. Stichler, C. Keller, W. Wurth, and D. Menzel, Phys. Rev. B **63**, 205419 (2001).
[31]M. Birgersson, C.-O. Almbladh, M. Borg, and J. Andersen, Phys. Rev. B **67**, 045402 (2003).
[32]W. Olovsson, C. Göransson, T. Marten, and I. A. Abrikosov, Phys. Status Solidi B **243**, 2447 (2006).
[33]B. V. R. Chowdari, K. L. Tan, and W. T. Chia, Solid State Ionics **53–56**(Pt. 2), 1172 (1992).
[34]S. Hampshire, J. Non-Cryst. Solids **316**, 64 (2003).
[35]S. Sakka, J. Non-Cryst. Solids **181**, 215 (1995).
[36]P. F. Becher, S. Hampshire, M. J. Pomeroy, M. J. Hoffmann, M. J. Lance, and R. L. Satet, Int. J. Appl. Glass Sci. **2**, 63 (2011).
[37]K. Momma and F. Izumi, J. Appl. Crystallogr. **44**, 1272 (2011).
[38]See supplementary material at http://dx.doi.org/10.1063/1.4904720 for structural data of all compounds encountered in this work and values of core level eigenenergies.